Neuron 54, 499–511, August 17, 2007 ©2007 Elsevier Inc. DOI 10.1016/j.neuron.2007.03.036

Representation of Spatial Goals in Rat Orbitofrontal Cortex

Claudia E. Feierstein,[1,2] Michael C. Quirk,[2] Naoshige Uchida,[2,3] Dara L. Sosulski,[2,4] and Zachary F. Mainen[1,2,*]
[1] Watson School of Biological Sciences
[2] Cold Spring Harbor Laboratory
1 Bungtown Road
Cold Spring Harbor, New York 11724

Summary

The orbitofrontal cortex (OFC) is thought to participate in making and evaluating goal-directed decisions. In rodents, spatial navigation is a major mode of goal-directed behavior, and anatomical and lesion studies implicate the OFC in spatial processing, but there is little direct evidence for coding of spatial or motor variables. Here, we recorded from ventrolateral and lateral OFC in an odor-cued two-alternative choice task requiring orientation and approach to spatial goal ports. In this context, over half of OFC neurons encoded choice direction or goal port location. A subset of neurons was jointly selective for the trial outcome and port location, information useful for the selection or evaluation of spatial goals. These observations show that the rodent OFC not only encodes information relating to general motivational significance, as shown previously, but also encodes spatiomotor variables needed to define specific behavioral goals and the locomotor actions required to attain them.

Introduction

The orbitofrontal cortex (OFC) is a subregion of the prefrontal cortex thought to be specialized for processing information about reward and punishment. Electrophysiological studies have shown that single neurons in the OFC respond selectively to appetitive or aversive stimuli, such as palatable or unpalatable foods (Thorpe et al., 1983; Tremblay and Schultz, 1999, 2000b). After learning, OFC neurons come to encode neutral stimuli that have been associated with such motivationally significant stimuli (Roesch and Olson, 2004; Rolls, 1996; Schoenbaum et al., 1998; Tremblay and Schultz, 1999, 2000a).

The OFC is widely believed to be involved in goal-directed decision-making (Cardinal et al., 2002; Damasio, 1994; Roberts, 2006; Rolls, 1996; Schoenbaum and Setlow, 2001; Schultz et al., 2000), but its specific function in goal-directed behavior is not well understood. A specific proposal is that OFC contributes to goal selection by encoding the abstract value of disparate potential options in a single currency (Arana et al., 2003; Montague and Berns, 2002; O'Doherty et al., 2001; Padoa-Schioppa and Assad, 2006). In contrast to pure representation of abstract incentive value or motivational significance, OFC could also have a direct role in representing concrete goals as targets of behavior, a function thought to be essential for goal-directed behavior (Dickinson and Balleine, 1994). Neurons in OFC do encode specific sensory features that distinguish different types of rewards (Rolls, 1996; Schoenbaum and Eichenbaum, 1995), and OFC lesions can affect learning based on sensory features that differentiate outcomes (McDannald et al., 2005). On the other hand, there is yet no electrophysiological evidence for encoding of actions or action-reward associations (Padoa-Schioppa and Assad, 2006; Schoenbaum and Eichenbaum, 1995; Tremblay and Schultz, 2000b; Wallis and Miller, 2003), as there is for the medial and lateral prefrontal cortex (Matsumoto et al., 2003) and striatum (Samejima et al., 2005).

In rodents, spatial navigation (including orientation, approach, and other locomotor behaviors) is the principal modality of goal-directed action, and orbitofrontal cortex is part of a network of areas implicated in spatiomotor processing. The ventrolateral subdivision of the OFC, area VLO, is directly connected to a number of areas concerned with spatial information processing, including direct reciprocal connections to the posterior parietal cortex (PPC), medial agranular cortex (Fr2) (Reep et al., 1996), and the medial prefrontal cortex (mPFC), through which it receives hippocampal input (Ferino et al., 1987; Reep et al., 1996). Consistent with this anatomy, lesion studies implicate OFC in the performance of tasks that involve spatial navigation. Ablating or inactivating the rat VLO impairs performance of an allocentric foraging task (Corwin et al., 1994), escape in the Morris water maze (Vafaei and Rashidy-Pour, 2004), and conditioned place avoidance (Vafaei and Rashidy-Pour, 2004). While there is electrophysiological evidence for the encoding of odor-place associations in the OFC (Lipton et al., 1999), there yet is no direct evidence for the specific representation of spatial or motor variables.

The aim of this study was to characterize neuronal activity in OFC in a spatial response task and to understand this area's possible contribution to the selection or evaluation of goal-directed choices. We hypothesized that orbitofrontal cortex may be important to representing spatial goals (defined as the locations to which locomotor behavior is directed) and possibly, in addition, the actions required to reach them. We used a two-alternative choice design in which different odor stimuli cued the availability of a water reward at one of two spatially distinct "goal" ports, requiring a spatial choice between these two goals in each trial. Although the appropriate choice varied from trial to trial depending on the odor cue, the average value of the rewards at the two ports was the same. This task design, along with the analysis of both correct and error trials, allowed direction or spatial encoding to be dissociated from both stimulus and outcome encoding. We found that in the context of

*Correspondence: zach@cshl.edu
[3] Present address: Center for Brain Science, Department of Molecular and Cellular Biology, Harvard University, Cambridge, Massachusetts 02138.
[4] Present address: Center for Neurobiology and Behavior, Columbia University, New York, New York 10032.

this task over half of OFC neurons encoded the direction of choice or the location of the goal. Moreover, a subset of neurons encoded both the direction and outcome (success or failure) of the choice. Therefore, in contrast to the idea of a pure valuation signal (Arana et al., 2003; Montague and Berns, 2002; Padoa-Schioppa and Assad, 2006; Roberts, 2006), neurons in the rat OFC encode specific spatial-motor variables required for the representation of goal locations and the responses required to obtain these goals.

Results

Task and Recordings

Five rats were trained to perform an odor-cued two-alternative choice discrimination task (Uchida and Mainen, 2003). The timing of events is depicted in Figure 1A for an example trial. A rat initiates a trial by entering the central odor-sampling port (*initiation*), triggering the delivery of one of two odors (*stimulus*). The rat responds by moving to one of two goal ports (*response*). A water reward is delivered for correct choices, while error trials are not rewarded, and no other feedback is provided (*outcome*). Therefore, trials were divided into four main behavioral epochs: *initiation*, *stimulus*, *response*, and *outcome* (see Experimental Procedures for definitions of these epochs).

Following training (1–2 weeks from the beginning of animal handling until reaching a performance accuracy of 85%), rats were implanted with a chronic electrode drive consisting of six independently adjustable tetrodes. During recordings, animals performed 62 to 452 trials per recording session (227 ± 119 trials/session, mean ± SD, n = 5 rats), and data were collected for 7 to 22 sessions per rat. Animals were well trained but did not perform perfectly. Performance accuracy for pure odors improved from 82% ± 7.0% (grand average of means ± SD, for all five rats) in the first recording session to 89% ± 2.6% in the last one. Compared to unimplanted animals (Uchida and Mainen, 2003), odor-sampling time (see Experimental Procedures) was similar (223 versus 255 ± 49 ms, grand average of medians), but movement time was somewhat slower (274 versus 386 ± 84 ms), probably due to some restriction of movement by the recording cable and headstage. Behavioral performance during recording sessions for one of the rats is shown in Figures 1B–1D (training sessions are not shown).

Electrode tracks were recovered after termination of the experiment using standard histological techniques (see the Supplemental Data available online). Recording locations were in three subregions of OFC: in ventrolateral orbitofrontal (VLO) and lateral orbitofrontal (LO) cortex and agranular insular cortex (AI) (Figure 2A). Cells were isolated offline using manual clustering methods (see Supplemental Data), and up to ten single units were isolated on individual tetrodes (mean 2.8 ± 2 units/tetrode). Figure 2B shows an example of a tetrode where two units were isolated. Only units with good isolation and recording stability across the session were included in the analysis.

The total data set consisted of 598 OFC single units. We used spike width to distinguish putative interneurons and pyramidal neurons (Figure 2C). In the population of single units recorded, 8% were classified as

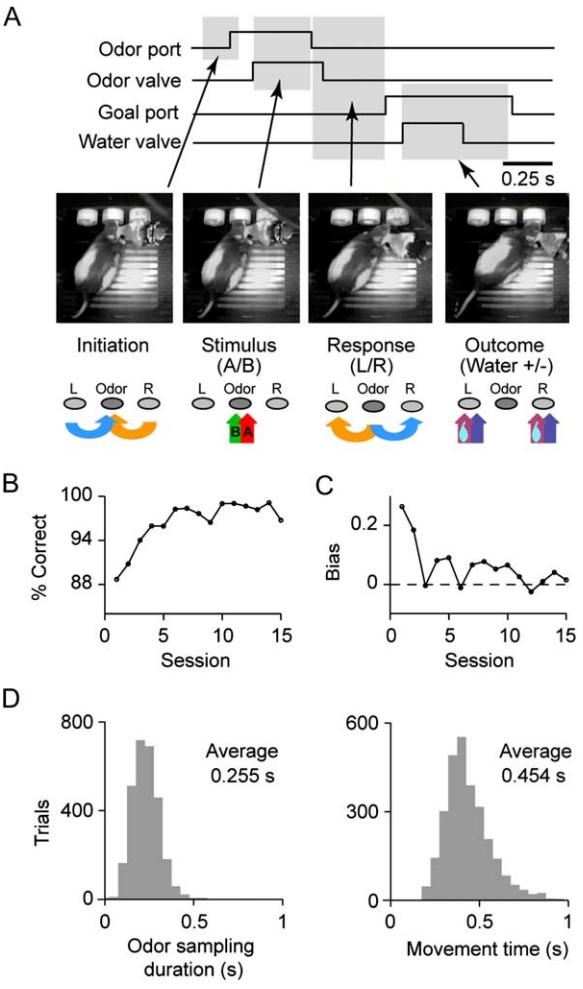

Figure 1. Two-Alternative Choice Discrimination Task

(A) Each trial was divided into four epochs: *initiation*, *stimulus*, *response*, and *outcome*. (Top) Schematic diagram of the timing of behavioral events in an example trial. Behavioral events are recorded using the interruption of the photobeams in the ports (timing of the rat responses) and signals opening the valves (timing of computer-triggered events). Gray-shaded boxes represent the boundaries of the trial epochs. (Middle) Frames of the rat performing the task, depicting the four behavioral epochs studied. (Bottom) Diagrams depicting the rat's location relative to the three ports (L, Odor, R) and the relevant variables in each of the epochs. *Initiation*: the rat enters the central port to initiate a new trial. *Stimulus*: the rat is at the central odor port and one of two odors (odor A, red arrow; odor B, green arrow) is delivered. *Response*: the rat moves from the central port to the left (orange arrow, leftward movement) or right (blue arrow, rightward movement) goal ports. *Outcome*: The rat is at one of the goal ports; for correct trials, a drop of water is delivered (purple arrow); for error trials, water reward is omitted (blue arrow). Schematics in subsequent figures follow the same conventions.

(B) Task performance. Accuracy (percent correct choices) changes over the course of the recording sessions; data shown for one of the rats.

(C) Choice (left/right) bias (see Experimental Procedures) across recording sessions for the same rat shown in (B).

(D) Odor sampling and movement times for the rat shown in (B) and (C). (Left) Distribution of *odor sampling duration* (OSD). (Right) Distribution of *movement time* (see Experimental Procedures). Grand average of median *odor sampling duration* and *movement time* across the 15 recording sessions are shown in the corresponding plots.

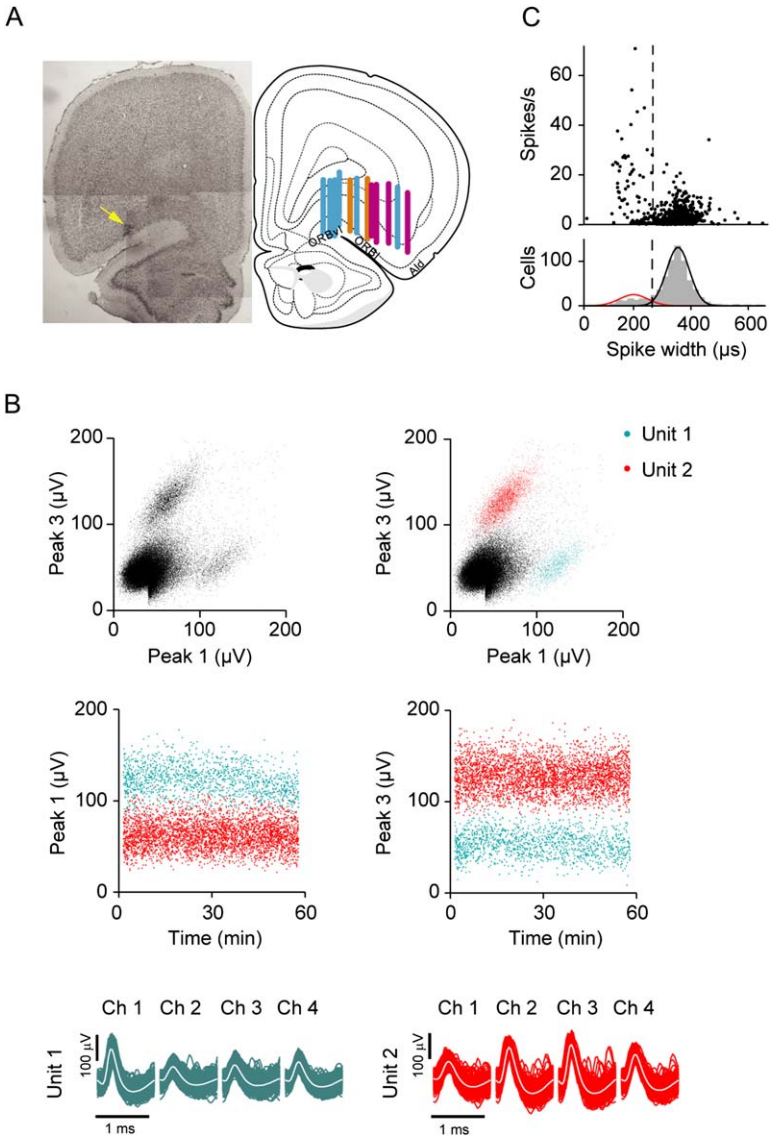

Figure 2. Recordings Sites, Unit Isolation, and Cell Classification

(A) Recording sites. (Left) Nissl-stained coronal section from one of the rats, showing a lesion site from one tetrode (yellow arrow). (Right) electrode tracks are overlaid on atlas section corresponding to 3.60 mm anterior to bregma (modified from Swanson, 1998). Note that recording locations ranged from +3.2 to +4.0, but are all shown on the +3.6 atlas section. Colored lines represent recording locations estimated from recovered electrode tracks. Each color indicates a different animal. ORBvl, ventrolateral OFC; ORBl, lateral OFC; AId, agranular insular-dorsal.

(B) Example of a tetrode where two units were isolated. (Top) The amplitude of the recorded waveforms is shown for two of the four channels. (Left) Scatter plot shows 10% of the triggered events recorded in the session. (Right) Points assigned to unit 1 (green) and unit 2 (red) and unassigned (black). Isolation distance (ID), unit 1, 34; unit 2, 54. (Middle) Spike amplitudes as a function of time. (Bottom) Spike waveforms for the two clustered units (unit 1, green; unit 2, red) as recorded in the four channels. For each unit, color traces show representative waveforms, and the white trace corresponds to the average waveform for the channel.

(C) Classification of neurons based on spike width. (Top) Scatter plot of spike width versus average firing rate for all isolated units (n = 598). Firing rates were calculated across the entire recording session. (Bottom) Distribution of spike widths. Gaussian fits to narrow-spiking units (red line, i.e., putative interneurons) and wide-spiking units (black line) are shown.

narrow spiking, putative interneurons (width < 260 μs). In this report we focus exclusively on the remaining 544 units, a population that includes both pyramidal neurons and other nonpyramidal, wide-spiking neurons.

Stimulus Representations

Odor selectivity has been previously reported in the LO and AId subregions of rat OFC (Schoenbaum and Eichenbaum, 1995). In our recordings, a relatively small population of OFC neurons discriminated between different odor stimuli. One of the most selective neurons encountered is shown in Figure 3A. This neuron responded strongly during the presentation of 1-hexanol, which was paired with left reward, and did not respond during the presentation of caproic acid, which was paired with right reward. To quantify selectivity, we use receiver operator characteristic (ROC) analysis to define a measure of how well the firing rate of the neuron can be used to classify the stimulus (or response direction or outcome; see Supplemental Data). The defined metric, *preference*, is proportional to the area under the ROC curve, but is scaled from −1 to 1, with 0 being nonselective (see Experimental Procedures). Population data for stimulus preference calculated during the *stimulus* period are shown in Figure 3B; the fraction of neurons showing significant preference ($p < 0.01$, based on a permutation procedure) for one of two odors was 14.5% (79/544 units).

In go/no-go paradigms in which one odor is associated with delivery of water reward at a specific spatial location while a second odor is associated with either punishment (Schoenbaum et al., 1999) or no water delivery (Schoenbaum and Eichenbaum, 1995) at the same location, apparent odor selectivity can result from selectivity for the reward value predicted by the stimuli. In the present design, the two odor cues were each associated with identical water reinforcers, but these reinforcers were delivered at two different goal ports. Thus, the identity of the odor presented at the beginning of a given trial is not predictive of the value of reward that could be expected at the end of that trial, but is predictive of the choice direction that will be rewarded or the location where reward will be available.

To better distinguish between odor selectivity and choice prediction, we trained animals to associate

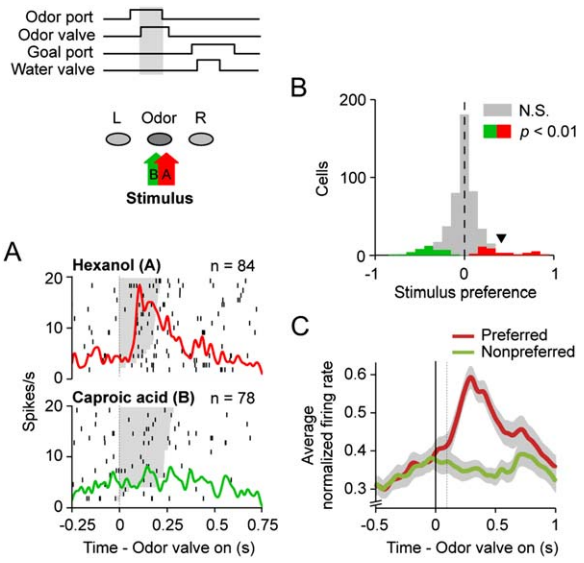

Figure 3. Stimulus Selectivity in Rat OFC

(A) Example of a stimulus-selective unit. Raster plots represent neuronal activity in individual trials (rows); each tick mark represents a spike. Trials for different stimuli were interleaved in the session but here are grouped according to stimulus identity. Twenty representative trials are shown in each raster plot, sorted according to *stimulus* period duration (gray-shaded area represents *stimulus* period). Only correct trials are included. Perievent histograms are overlaid on raster plots and were computed for each group of trials (n indicates the number of trials of a given type) and smoothed with a Gaussian filter (σ = 10 ms). Raster plots and histograms are aligned to odor valve opening (time = 0). (Top) Trials in which 1-hexanol was presented (red). (Bottom) Trials in which caproic acid was presented (green).

(B) Stimulus selectivity for the population of OFC cells. Stimulus preference was calculated using an ROC analysis (see Experimental Procedures). Positive values correspond to higher firing rate for stimulus A (left rewarded) trials; negative values correspond to cells with higher firing rate for stimulus B (right rewarded) trials; 0 is nonselective. Color bars, significant selectivity with $p < 0.01$ based on a permutation procedure; red, cells selective for stimulus A; green, cells selective for stimulus B. Gray bars, not significant. The arrowhead indicates the value of the example cell in (A).

(C) Time course of stimulus selectivity. Peak normalized firing rate was averaged across stimulus-selective cells (defined as in [B]) for the preferred (red) and nonpreferred (green) stimulus conditions and is plotted aligned to odor valve opening (time = 0). Note that there is an empirically estimated odor latency to reach the epithelium of 100 ms after odor valve onset (dotted line; see Experimental Procedures). Shading represents 1 SEM.

multiple odors with water at each goal port. Specifically, four or six odors were randomly interleaved, with half of the odors assigned to the right and half to the left goal ports. If OFC neurons encode stimulus information, then units ought to discriminate not only between left/right response categories but also among odors within a category. A total of 57 neurons were recorded during multiple-odor discrimination sessions; of those, seven showed "odor selectivity" when selectivity was calculated between left/right response categories (see Supplemental Data). The fraction of category-selective neurons was similar to the fraction of stimulus-selective units observed in two-odor sessions (12.3% versus 14.5%; $p > 0.5$, χ^2 test). When odors within a response category were compared, only 2 of 57 units showed significant selectivity, suggesting that OFC neurons primarily encode the behavioral response category rather than uniquely encoding each stimulus.

For the unit illustrated in Figure 3A, selectivity peaked around the end of the *stimulus* period, i.e., the time of the choice, and continued into the *response* period. To estimate the time course of selectivity of the population, we selected all the units showing a significant stimulus preference, calculated their peristimulus time histograms (PSTHs), normalized each one according to the peak firing rate, and averaged them together. The peak-normalized average PSTH shows a short-latency onset, a rise of approximately 100–130 ms (after accounting for the experimentally estimated odor delay of 70–100 ms, see Experimental Procedures), and a peak near the end of the *stimulus* period (Figure 3C). Thus, odor information was processed by the OFC sufficiently rapidly to participate, in principle, in selection of response direction.

Behavioral observations suggest that the rat has already chosen a response direction by the time it leaves the odor port (Uchida and Mainen, 2003); therefore, neuronal correlates of the decision should be found during the stimulus period. One signature of the direct participation of OFC in an animal's choice of action would be the ability to predict from neuronal activity the rat's choice direction before responses are initiated (i.e., during the *stimulus* period). We calculated *choice probability* (Britten et al., 1996), the probability of correctly predicting the rat's choice given the neuronal firing rate on each trial. This analysis uses an ROC-based metric to compare left and right trials for a given stimulus (note that this means comparing correct and error trials for each stimulus; see Experimental Procedures). Choice probability for the population of cells was 0.57 ± 0.03; few cells (5.8% or 10/172 units) showed choice probability that significantly differed from chance. Thus, a small population of OFC neurons carried information about the animal's choice before response initiation.

Encoding of Choice Direction and Goal Location

We next examined selectivity for the direction of the choice the rat made during the leftward or rightward movement from the odor port to one of the goal ports (*response* period; see Figure 1A). While coding of response direction has not been previously described in the OFC of rats or monkeys, direction selectivity was the most robust type of tuning we encountered in the two-alternative choice task. Figure 4A shows an example of a unit with robust direction selectivity characteristic of one group of neurons we encountered. This group of neurons showed very low background firing rate (<1 Hz) and robust responses (10 to >50 Hz), with a peak during the movement from the odor port to the goal port. A large fraction of OFC neurons showed significant selectivity for response direction during the *response* period (221/544 cells, 41%). While we recorded exclusively from the left OFC, selectivity for direction was symmetric for left and right directions (mean direction preference = 0.02 ± 0.03, n = 221 selective cells, 117 left-selective cells, 104 right-selective cells; see Figure 4B). Some direction-selective cells maintained their selectivity upon entry into the goal port, and a subset of left/right-selective neurons fired only after entry into the

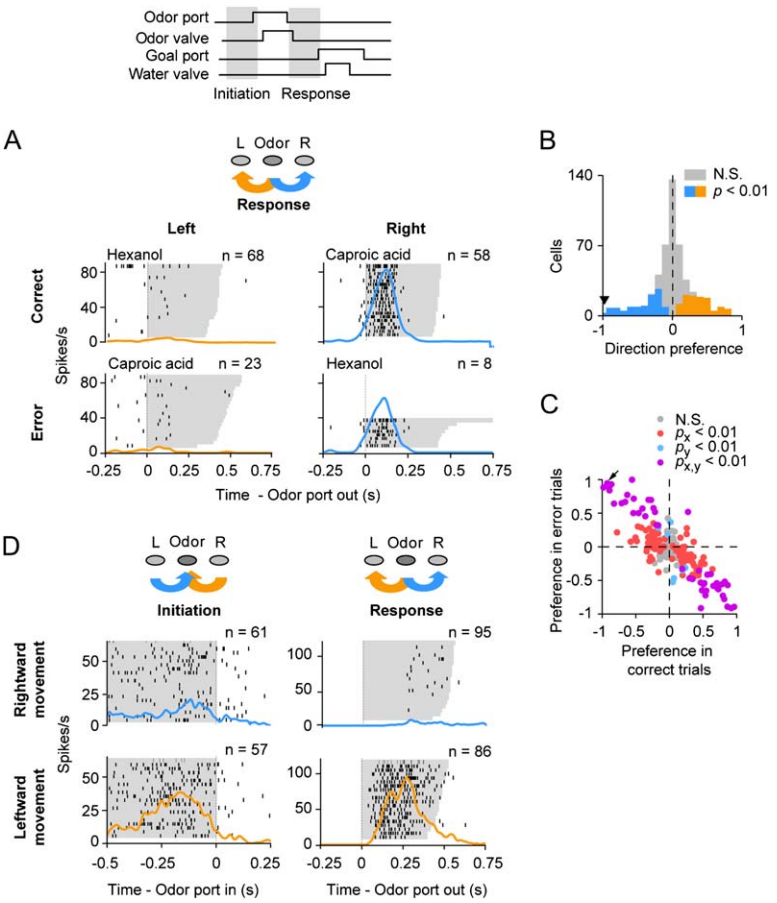

Figure 4. Neurons in OFC Were Selective for Spatial Location/Direction

(A) Example of a direction-selective neuron. (Raster plots) Trials are grouped according to stimulus and direction. Trials are sorted according to movement time (gray-shaded area represents *response* period). Raster plots and histograms are aligned to movement out of the odor port (odor port out). (Left column) Trials in which the rat moved to the left (orange). (Right column) Trials in which the rat moved to the right (blue). The upper plots correspond to correct trials, while the lower plots correspond to error trials.

(B) Population histogram of response direction preference. Direction (L/R) preference was calculated during the *response* period using ROC analysis. Color bars, significant selectivity ($p < 0.01$); orange, selective for left movement; blue, selective for right movement; gray, no significant selectivity. Arrowhead indicates the example cell in (A).

(C) Population analysis of direction selectivity. Stimulus preference (A/B) in correct trials (x axis) is plotted against preference (A/B) in error trials (y axis). Each point represents a cell, color-coded for significance ($p < 0.01$ for preference in correct trials, in error trials, or both; see legend). Note that points lying on the descending ($x = -y$) diagonal correspond to direction-selective cells.

(D) Cells were tuned for direction of movement at different points in the trial sequence. (Raster plots, right column) Trials are grouped according to direction of movement during the *response* period (blue, rightward movement; orange, leftward movement) and sorted according to movement time. Gray-shaded area represents the *response* period. Raster plots and histograms are aligned to movement out of the odor port (odor port out). (Raster plots, left column) For the same cell, trials are now grouped according to the previous trial's choice, i.e., direction of movement during the *initiation* period (blue, rightward movement; orange, leftward movement). Raster plots and histograms are aligned to movement into the odor port (odor port in). Gray shaded area shows the movement back from the goal ports. Both correct and error trials are included. Note that this cell fired selectively for leftward movements in both phases of the task.

goal port (Figure 5A). Overall, 35% of the cells (189/544) were selective for left/right location while the rat was at the goal port. Population data for left/right preference during the *outcome* period (i.e., while the rat is at the goal port) are shown in Figure 5B. Altogether, 56% of cells were left/right tuned in either the *response* or *outcome* periods.

Do direction-selective neurons reflect tuning for the preceding odor stimulus? If firing during the *response* or *outcome* periods reflected an odor memory, then left- or right-selective neurons should also be specifically tuned to a given preceding odor. For each session using multiple odors, we calculated stimulus selectivity among trials sharing a response direction (see Supplemental Data). In some cases, there was a statistically significant modulation by odors within a response category: 23% (9/39) during the *response* period and 8% (3/36) during the *outcome*. However, this modulation was in each case much weaker than selectivity across categories. Examples of neurons tested with multiple odors are shown in Figure 9A and Figure S2; note that these neurons did not discriminate among odors in the response category.

Although this analysis suggests that direction tuning is not a simple result of stimulus selectivity, by comparing trials in which the animal made correct and incorrect choices, we could dissociate stimulus and direction and test whether the firing of these neurons tracked the direction of the response rather than the identity of the preceding odor stimulus. Examination of error trials for the unit in Figure 4A illustrates this point. This neuron responded strongly in correct caproic acid trials and error 1-hexanol trials, which shared a movement direction (right), and weakly in correct 1-hexanol trials and error caproic acid trials, which also shared a movement direction (left). Across the population this can be seen by plotting selectivity in correct trials versus selectivity in error trials (Figure 4C). In this plot, neurons that are stimulus selective should fall along the line $x = y$, while those that are direction selective should fall along the $x = -y$ diagonal. It can be seen that the population of selective units falls along the latter diagonal.

The interpretation that direction-selective firing reflected choice direction and not stimulus memory is further supported by the observation that a population of direction-selective neurons fired not only when exiting the odor sampling port but also when moving toward the odor sampling port (*initiation*), that is, before odor presentation. These neurons fired for movements sharing a direction but occurring at different spatial locations

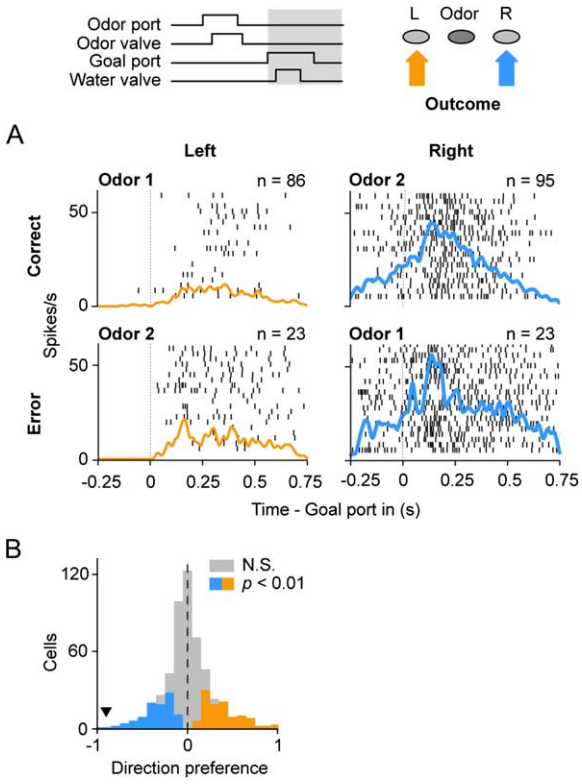

Figure 5. OFC Cells Were Selective for Port Location

(A) Example of a cell that encoded goal port location. Trials are grouped according to choice (port location) and further divided according to trial outcome. Trials are displayed in temporal order. Raster plots and histograms are aligned to entry into the goal port. (Left column) Left choice trials: the rat's snout entered the left goal port (orange). (Right column) Right choice trials: the rat's snout entered the right goal port (blue).

(B) Population histogram of port location preference. Side (L/R) preference was calculated during the *outcome* period for correct trials only. Color bars, significant selectivity ($p < 0.01$); orange, selective for left port; blue, selective for right port; gray, no significant selectivity. Arrowhead indicates the example cell in (A).

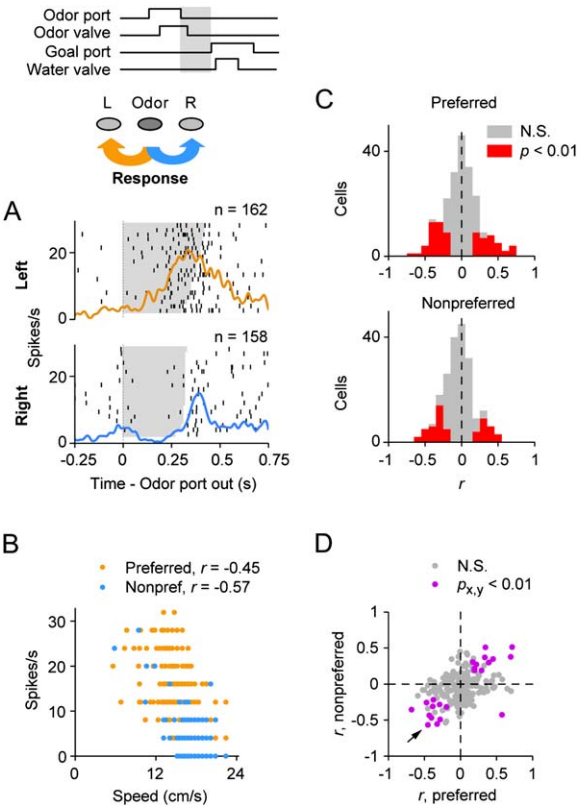

Figure 6. Speed of Movement Modulates Activity of Direction-Selective Neurons

(A) Example of a L/R-selective neuron that showed further modulation by speed of movement. Rasters and PSTHs show trials grouped according to direction of movement during the *response* period. Trials are sorted according to movement time (gray-shaded area represents *response* period). Raster plots and histograms are aligned to movement out of the odor port (odor port out). (Top) Trials in which the rat moved to the left (orange). (Bottom) Trials in which the rat moved to the right (blue).

(B) Correlation of speed and firing rate during the *response* period. For the example cell in (A), speed of movement (see Experimental Procedures) is plotted against firing rate. Each point represents a trial, color coded for trials of this neuron's preferred (orange) and nonpreferred direction (blue). Note that speed and firing rate are negatively correlated for both trial types (correlation coefficient r for preferred −0.45, for nonpreferred −0.57). Firing rates look quantized due to the use of a window of fixed length for calculating the firing rate.

(C) Population distribution of correlation coefficients (r) for firing rate versus speed during the *response* period. Distribution of correlation coefficients for movement in the cell's preferred direction (top) and for movement in the cell's nonpreferred direction (bottom). Significance was based on t statistics.

(D) Speed/firing rate correlations (r) for the preferred and nonpreferred direction coincide for some direction-selective cells. Scatter plot showing the correlation coefficient for speed versus firing rate for the preferred (x axis) and nonpreferred (y axis) directions of movement. Each point corresponds to one direction-selective cell. For some cells, speed and firing rate were significantly correlated ($p < 0.01$ based on t statistics) for both the preferred and nonpreferred directions (purple). Note that some cells showing a significant correlation for only one of the directions of movement are shown in gray.

and at different points in the behavioral sequence. Figure 4D illustrates a unit that fired when the animal was leaving the center port to the left and also when it was leaving the right goal port heading left to return to the odor port. Of the 221 units showing direction selectivity during the movement from odor port to goal port, 41 (19%) also showed significant direction selectivity during the movement from the goal port back to the odor port. Such tuning cannot arise from odor selectivity and could be parsimoniously explained as a representation of an orientation or direction of movement rather than a location.

The form of direction selectivity we observed is consistent with both the encoding of head direction or of some parameter of the turn and approach movement. To further explore the latter possibility, we tested whether firing rates of direction-selective neurons correlated with speed of movement. Indeed, 34.4% of this population (76/221) showed a significant correlation between firing rate and speed in their preferred directions (see Experimental Procedures). An example neuron exhibiting a negative correlation between movement speed and firing rate is shown in Figures 6A and 6B. The distribution of correlation coefficients for the population of direction-selective cells is shown in Figure 6C.

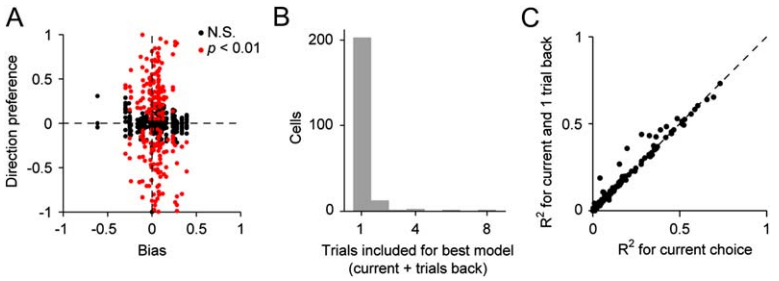

Figure 7. Direction Selectivity Is Not Explained by Choice History

(A) Direction preference does not correlate with choice bias. Direction (L/R) preference is plotted, for each cell, as a function of choice bias (see Experimental Procedures) in the session in which it was recorded. Red, cells that showed significant ($p < 0.01$) direction selectivity; black, no significant selectivity (N.S.).

(B and C) Summary of multiple linear regression analysis. Multiple linear regression was used to examine the dependence of the firing rate in the *response* period on both the current choice direction and the choice direction in the past *n* choices (see Supplemental Data for details). (B) Distribution of the number of trials included in the best multiple regression model for each cell in the population of direction-selective units. (C) Comparison of R^2 for the regression models including only the current trial's choice and models including both the current and the previous trials' choices. Each dot represents a cell. Note that including the previous trial results in an improved model only for a few of the direction-selective cells (the cells that are above the diagonal).

Note that the speed tuning for the preferred and nonpreferred directions in the population of direction-selective cells showed the same sign of correlation (Figure 6D).

Although together the above observations strongly suggest that OFC neurons encode a spatial or motor representation, a possible confound in this interpretation could arise due to choice (left/right) bias. If OFC units were strongly tuned for expected value and the relative value of left and right choice ports varied systematically (despite steps taken to maintain equal reward values at the two ports; see Supplemental Data and Figure S3), then, in principle, such tuning could influence left/right spatial selectivity. In this scenario, left/right asymmetries in port value might be reflected in a left/right choice bias. Most rats did in fact show a small overall left/right choice bias (Figure 1C), but direction selectivity was not correlated with this bias (Figure 7A). Moreover, multiple regression analysis using current and past trial choice directions (the latter being taken as a measure of choice bias; see Supplemental Data for details) showed that for all but a handful of direction-selective cells (8/221, or 3.6%) only the current trial choice contributed significantly to explaining trial-by-trial variance in firing rate during the *response* period (Figures 7B and 7C and Figure S4). Thus, left/right tuning of OFC neurons does not appear to result from value selectivity reflected in choice bias.

Outcome Representations

Finally, we analyzed activity during the trial outcome, the delivery of water or its omission. Selectivity of OFC neurons for such motivationally significant events has been proposed to represent either encoding of salient stimuli themselves or evaluation of predictions concerning the delivery of those stimuli (Thorpe et al., 1983; Tremblay and Schultz, 2000b). More OFC units (75%; see Supplemental Data) showed response modulation during the trial *outcome* period than any other epoch, and many responsive cells were selective for the type of outcome (29%, or 133/463 cells during a 500 ms epoch following water delivery or its expected delivery). Figure 8A shows an example of a cell that fired selectively for error trials at around the time that water would have been delivered. Other neurons responded more strongly during correct than error trials. At the population level, more OFC neurons were selective for reward omission than reward delivery (mean outcome preference = −0.21 ± 0.03, for 133 outcome-selective units). This can be seen in a histogram of outcome preference (Figure 8B). It is important to note that firing to reward omission is very unlikely to

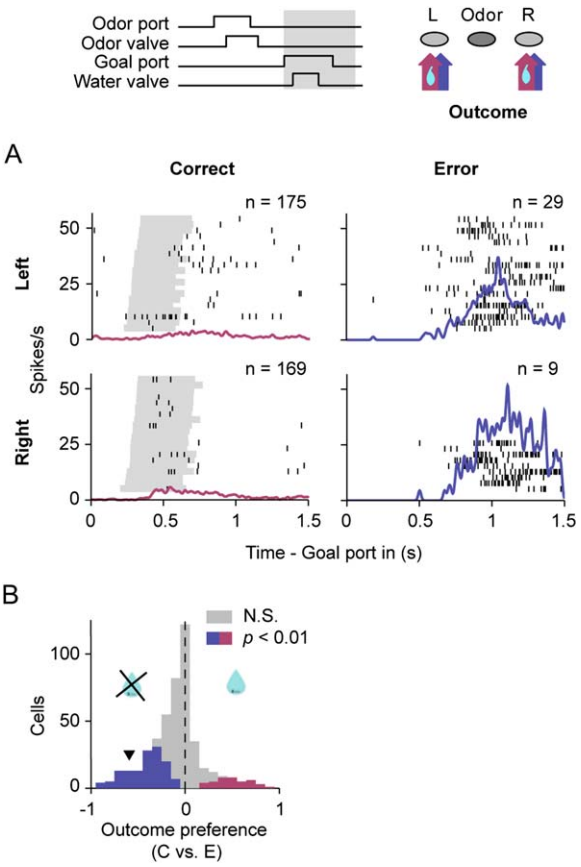

Figure 8. Outcome Selectivity

(A) Example of an outcome-selective neuron. Trials are grouped according to trial outcome (water delivery or omission) and further divided according to choice direction. Correct trials are sorted according to delay to water delivery; error trials are displayed in temporal order. Gray-shaded area represents the duration of water valve opening for correct trials only. Raster plots and histograms are aligned to entry in the goal port. (Left column) Correct trials, purple. (Right column) Error trials, blue.

(B) Population histogram of outcome preference. Outcome preference was calculated using an ROC analysis comparing correct and error trials. Color bars, significant selectivity with $p < 0.01$; purple, selective for correct trials, blue, selective for error trials; gray bars, not significant. Arrowhead indicates the example cell in (A).

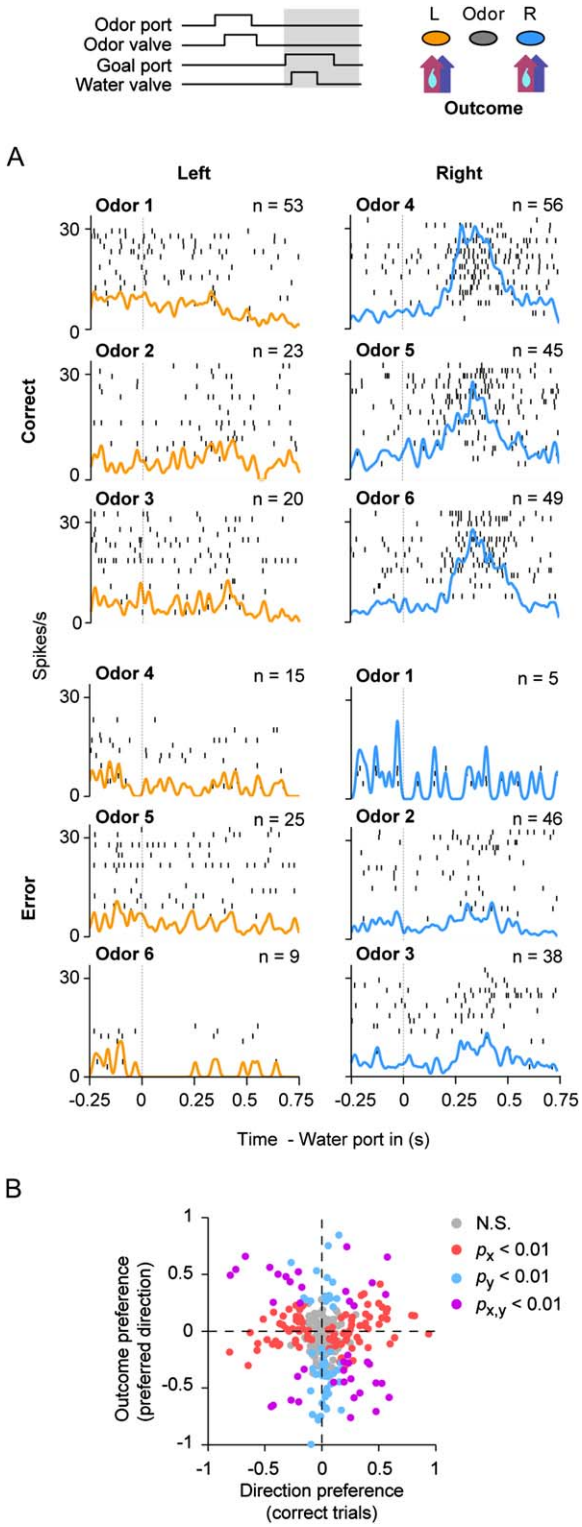

Figure 9. Conjunctive Coding of Direction/Location and Outcome

(A) Example of a single unit that responded to the combination of outcome and location. This unit was recorded during a six-odor discrimination experiment. Trials are grouped according to choice (port location) and further divided according to stimulus identity. Trials are displayed in temporal order. Raster plots and histograms are aligned to entry into the goal port. (Left column) Left choice trials (orange). (Right column) Right choice trials (blue). The six upper plots correspond to correct trials, whereas the six lower plots correspond to error trials. Odor 1, 1-hexanol; odor 2, butyric acid (1/10); odor 3, S(+)-2-octanol (1/10); odor 4, caproic acid (1/10); odor 5, (-)-carvone (1/10); odor 6, amyl alcohol (1/10).

(B) OFC neurons integrate spatial and outcome information. Population scatter plot of direction preference (L/R selectivity in correct trials) versus outcome preference (C/E) for the cell's preferred direction during the *outcome* period. Each point corresponds to a cell, color coded for significance (see legend); note that cells in purple are selective for both the location of the goal port and the outcome of the trial. Arrow shows the example cell in (A).

be a direct sensory response, as there was no sensory event (valve click, error signal, etc.) for the neuron to encode.

The preceding analyses established that many OFC neurons encode response directions or goal locations, but only a small fraction of neurons appear to participate in goal selection (anticipate the decision), as they should if OFC were actively guiding decisions. If OFC is instead primarily monitoring or evaluating decision outcomes, then neurons representing choice direction or goal location might be sensitive to the outcome of individual trials. Examination of both left/right selectivity and correct/error selectivity during the *outcome* period showed that a subset of OFC units indeed jointly encoded outcome and goal location. Figure 9A shows an example of a neuron with strong location (right goal port) and outcome (water delivery) preference. Figure 9B shows joint outcome/direction selectivity for the population of OFC neurons. For this analysis, we first determined the preferred direction of each unit (when multiple odors were used, trials sharing a correct response direction were considered as a group). Then for trials of the preferred location, we compared activity for correct and error trials. The scatter plot in Figure 9B shows the result of this analysis, where left/right preference is plotted against outcome preference. Of the direction-selective cells, 30% (40/134 cells for which enough error trials were available) were also selective for the outcome at the preferred location. Conversely, of the outcome-selective neurons, 34% (36/106 cells) were direction selective as well. Thus, OFC units combined information about the location of the reward port or the direction of preceding response used to reach it and the outcome associated with the choice.

Discussion

Previous electrophysiological and imaging studies have demonstrated that neurons in the OFC encode the subjective value or motivational significance of stimuli (Padoa-Schioppa and Assad, 2006; Roesch and Olson, 2004, 2005; Schoenbaum et al., 1998, 1999, 2003b; Tremblay and Schultz, 1999; Wallis and Miller, 2003). Here we demonstrate that the OFC in the rodent encodes spatial variables that define important objective properties of behavioral goals. Neurons in rodent OFC therefore do not simply encode the economic valuation of behavioral options (Montague and Berns, 2002; Padoa-Schioppa and Assad, 2006) but represent the specific properties of goals (i.e., location) and actions required to obtain them (i.e., choosing the appropriate heading to reach a desired location). In this way, OFC representations fulfill essential requirements of

goal-directed behavior as suggested by animal learning theory (Dickinson and Balleine, 1994).

Encoding Goal Locations and Response Directions

In this two-alternative spatial response task, more than half of OFC neurons showed selectivity for response direction; this selectivity was more prominent than for any other task variable. Neurons selective for response direction fired during three phases of the task: movement from odor port to goal port, while the rat was at the goal port, and during the movement from the goal port back to the odor port. The firing of some neurons was consistent with a representation of position. However, the robustness of firing during the movement period (firing rates >50 Hz), the existence of cells that fired during movements sharing a direction but not a location (see Figure 4D), and the prominent correlation between movement speed and firing rates suggest a locomotor rather than a purely spatial representation.

Our description of the encoding of variables related to response direction and goal location in OFC is consistent with and extends previous work on OFC representations. A series of studies by Schoenbaum and colleagues (Schoenbaum et al., 1998, 1999, 2003b; Schoenbaum and Eichenbaum, 1995) using a go/no-go task focused on the representation of outcome-predictive information during the stimulus and prereward delay periods and used a single goal location. A study by Lipton et al. (1999) used four odor/water ports, but because each odor was presented and rewarded at a fixed spatial location, the representation of spatial position was not dissociated from the representation of odor identity. By dissociating odor stimuli from choice direction and outcome using error trial analysis, we have shown that spatiomotor information is explicitly represented in OFC.

A number of groups have examined neural activity in monkey OFC and have either not reported evidence for spatial or motor representations (e.g., Thorpe et al., 1983; Wallis and Miller, 2003) or reported the absence of such selectivity (Padoa-Schioppa and Assad, 2006; Tremblay and Schultz, 2000b). Several factors could account for the difference between these findings and the present results. First, in the tasks used in the monkey studies, motor responses consisted of eye movements (Padoa-Schioppa and Assad, 2006; Wallis and Miller, 2003) or lever reaching (Tremblay and Schultz, 2000b), which only indirectly resulted in delivery of liquid reward through a single mouth tube. Thus, these studies did not use spatially distinct goals (reward locations) or approaches to those goals, as we did in the present study. Moreover, in the studies where monkeys responded with saccades (Padoa-Schioppa and Assad, 2006; Wallis and Miller, 2003), spatial selectivity could have been missed because spatial receptive fields were not mapped. Alternatively, apparent differences between rodent and primate OFC function may reflect imprecise knowledge of the homology between different subregions of prefrontal cortex across the two species (Carmichael and Price, 1994; Öngür and Price, 2000; Preuss, 1995; Uylings et al., 2003). It is also possible that rodent OFC plays a more integrated role in spatial cognition, combining stimulus, response, and outcome representations, as, for example, the primate dorsolateral PFC does for eye movements (e.g., Kobayashi et al., 2002; Matsumoto et al., 2003; Wallis and Miller, 2003).

The Orbitofrontal Cortex within a Network for Spatial Navigation

The representation of spatial and motor variables in rat OFC is consistent with anatomical and lesion data in this species. The rodent OFC, especially the ventrolateral region (VLO), where most of our recordings focused, is anatomically situated within a network of brain regions that process spatiomotor information, including the posterior parietal cortex and medial agranular cortex (Reep et al., 1996). OFC lesions in rats not only impair outcome reversals (McAlonan and Brown, 2003; Schoenbaum et al., 2002; 2003a) and devaluation (Gallagher et al., 1999; Pickens et al., 2003) but also produce deficits in spatial navigation tasks (Kolb et al., 1983), and area VLO is particularly critical to the latter effects (Corwin et al., 1994; Vafaei and Rashidy-Pour, 2004). Furthermore, unilateral VLO lesions produce a form of spatial neglect (King et al., 1989).

While encoding of spatial and motor variables related to the position or heading of an animal had not been reported in OFC, correlates of spatial navigation have been observed in many regions of the rodent brain. In addition to the better-known hippocampal place cells (O'Keefe and Nadel, 1978), thalamic head direction cells (Taube, 1998), and entorhinal grid cells (Hafting et al., 2005), spatial representations have been reported in cortical areas, including the subiculum (Cacucci et al., 2004; Sharp, 1999), sensorimotor cortex (McNaughton et al., 1994), posterior parietal cortex (McNaughton et al., 1994; Nitz, 2006), retrosplenial cortex (Chen et al., 1994a, 1994b; Cho and Sharp, 2001), and mPFC (Hok et al., 2005; Hyman et al., 2005). Areas strongly associated with spatial encoding, such as the hippocampus, also appear to encode variables related to behavioral salience (Eichenbaum et al., 1987). Thus, it will be an important challenge to determine how various functions involved in spatial navigation are parceled out among these areas.

Monitoring Rather Than Executing Goal-Directed Choices

OFC could perform an executive function in decision-making by selecting among alternative goals or by selecting responses associated with specific goals. While many stimulus-selective units appeared to encode primarily response category or associated goal location (rather than odor identity), choice probability analysis showed that only a small fraction of units (5.8%) anticipated the choice direction before motor initiation. This contrasts with, for example, results in primate dorsolateral PFC during a choice task where neurons reflect an upcoming motor response in anticipation of its execution (e.g., Leon and Shadlen, 1999; Wallis and Miller, 2003). Thus, while goals and goal-directed responses are represented in the OFC, this area does not appear to be strongly participating in goal or action selection in the context of our task. We tentatively attribute this result to the fact that goal port locations and outcomes were fixed and the odor-location associations were already well learned during recording. Based on results from lesion studies (Gallagher et al., 1999; Izquierdo et al., 2004; McAlonan and Brown, 2003; Schoenbaum

et al., 2002), we would expect that choice-predictive neurons will be more prominent in OFC when outcome value or stimulus-response-outcome contingencies change (e.g., in devaluation or reversal tasks). OFC might also play a stronger role in goal or action selection during task learning or during the acquisition of new odor-location (Lipton et al., 1999) or odor-response associations.

While OFC does not appear to be mainly involved in selecting goal-directed spatial responses in this task, it nevertheless contains a rich representation of task variables consistent with a function in monitoring responses and their outcomes. Of particular importance in this function is the large subset of OFC neurons that selectively encoded individual trial outcomes. Some outcome-selective neurons appeared to encode water delivery (e.g., Figure 9A). Insofar as water acted as a reinforcer, these responses could reflect a form of "value" (as opposed to sensory) coding, although we did not establish this directly. Other outcome-selective neurons responded with an increase in firing rate on error trials at the time when water reward was expected (Figure 8). Such reward omission responses might reflect encoding of reward prediction errors, as described previously in OFC (Thorpe et al., 1983; Tremblay and Schultz, 2000b) and posterior cingulate cortex (McCoy et al., 2003). Given the high performance of the animals during our recordings, error trials represented a larger deviation from expected outcome than correct trials, which could explain the bias in the population for error-selective units (Figure 8B). Whether these responses are quantitatively proportional to the difference between actual and predicted outcome (the prediction error in reinforcement learning theory), remains to be addressed. Outcome prediction error responses could serve to trigger learning (McCoy et al., 2003; Rescorla and Wagner, 1972) or alter decision-making following changes in outcome value or contingency.

Integration of Outcome and Location Information

Rather than reflecting a global abstract signal or reward attainment or prediction error, individual outcome-encoding OFC neurons were also selective for the location of the outcome. It is on the basis of this additional selectivity for an important objective property of the outcome—its location—that we consider OFC neurons to be encoding properties of behavioral goals rather than abstract signals related to subjective value alone. Location is a critical component of a goal representation because it defines attributes of a reward critical to representing it as a target of goal-directed action (Dickinson and Balleine, 1994).

This finding has significance in the context of reinforcement learning (RL) theory (Sutton and Barto, 1998), especially for beginning to clarify the possible role of the OFC in this framework (Hasselmo, 2005; Koene and Hasselmo, 2005). In particular, the existence of joint location-outcome-selective neurons suggests that OFC contains a representation of "state values," a concept that is central to RL. As to whether OFC participates as "actor" as well as "critic" in RL and whether it contains a representation of "state-action values" (as used in some variants of RL), our data are less definitive. Although, as noted above, direction-selective neurons suggest an action representation, in spatial tasks state (location) and action (approach to a location) are difficult to distinguish. Thus, it is possible that OFC is concerned solely with representing states and their value, while action policy learning and selection are carried out in other brain areas. Nevertheless, the existence of choice-predictive neurons, although few in number, indicates that OFC has the capacity for selection of spatial goals and might drive spatial choice selection under some circumstances.

Also, in the context of reinforcement learning, it is interesting to note that our results and others' (Rosenkilde et al., 1981; Thorpe et al., 1983; Tremblay and Schultz, 2000b) are consistent with the representation in OFC of a temporal difference prediction error signal during trial outcome, similar to that carried by the dopamine system (Schultz, 2002). However, in contrast to dopamine neurons, OFC neurons responded to *omission* of predicted rewards with an *increase* rather than a *decrease* in firing. Thus, OFC neurons might encode a quantity related to the *absolute value* of reward prediction error, as previously proposed for posterior cingulate cortex (McCoy et al., 2003). Such a term is similar to a formal definition of salience posited in animal learning theory (Pearce and Hall, 1980). Maps of stimulus salience have been proposed to exist in the parietal cortex (Gottlieb et al., 1998) and cingulate cortex (Dean et al., 2004) in primates. Further work is needed to establish the quantitative nature of OFC outcome signals, how they relate to spatial maps, and how they impact learning.

Experimental Procedures

See Supplemental Data for detailed procedures.

Animal Subjects and Behavioral Task

Rats had free access to food, but water was restricted to the behavioral session and ~15 additional min; drinking time was adjusted to maintain the rats at 85% of their free-drinking weight. All procedures involving animals were carried out in accordance with NIH standards and approved by the Cold Spring Harbor Laboratory Institutional Animal Care and Use Committee.

Behavioral training and testing were conducted as described in Uchida and Mainen (2003). The behavioral setup consisted of a box with a panel containing three ports equipped with infrared photodiode and phototransistor; interruption of the beam signaled that the rat had introduced its snout into the port. Odors were mixed with pure air to produce a 1:20 dilution at a flow rate of 1 l/min using a custom-built olfactometer (for detailed description see Uchida and Mainen, 2003). Delivery of odors and water reinforcement were controlled using computer data acquisition hardware (National Instruments) and custom software written in MATLAB (MathWorks, Natick, MA).

Rats were trained and tested on a two-alternative choice discrimination task as follows. Rats initiated the behavioral sequence by entering the odor-sampling port (Figure 1A), which triggered the delivery of an odor with a random delay of 0.2–0.5 s. In the two-odor variant of the task, rats were presented with either one of two odors; each odor signaled that water was available in one of the two goal ports. Some rats were trained on two variants of the task: a multiple-odor discrimination task using four or six odors or a binary-mixture discrimination task described elsewhere (Uchida and Mainen, 2003).

For correct choices, water was delivered with a random delay of 0.2–0.5 s from entry into the goal port. The system was calibrated regularly to ensure that equal amounts of water were delivered at both ports (see Supplemental Data and Figure S3 for calibration data). Behavioral sessions during recording consisted of 250 to 400 trials, spanning 45 to 75 min.

Surgery and Recordings

Each rat was implanted with a custom-made multielectrode drive in the left hemisphere in orbitofrontal cortex (3.5 mm anterior to bregma, 2.5 mm lateral to midline). Rats were allowed to recover for 5–7 days before resuming water restriction and starting the recordings. During that period, tetrodes were gradually lowered to reach OFC. Electrode placements were estimated by depth and later confirmed with histology.

Extracellular recordings were obtained using six independently adjustable tetrodes for recording. Individual tetrodes consisted of four twisted polyimide-coated nichrome wires (H.P. Reid, Inc., Palm Coast, FL; single-wire diameter 12 μm, gold plated to 0.25–0.35 MΩ impedance). Electrical signals were amplified and recorded using a multichannel acquisition system (Cheetah system, Neuralynx, Tucson, AZ). Multiple single units were isolated offline by manually clustering spike features derived from the sampled waveforms using MCLUST software (A.D. Redish). Recordings were obtained for 2–4 weeks with electrode depths adjusted on each recording day so as to sample an independent population of cells across sessions.

Behavioral Analysis

Performance was measured in two ways: accuracy and choice bias. *Accuracy* was defined as the percent correct choices (over the total number of correct and error trials; error trials were defined to include only trials in which an incorrect response was made, excluding from the analysis trials in which the rats made no choice). *Choice bias* for each session was calculated as follows: *choice bias* = $(n_{left} - n_{right})/(n_{left} + n_{right})$, ranging from −1 to 1, with 0 meaning no choice bias. *Odor sampling duration* was defined to designate the window of time the rat was exposed to the odor stimulus. The *stimulus* period (see below) starts at the opening of the odor valve and ends with the movement of the rat's snout out of the odor port. However, there is a delay due to valve latency and a delay for the odor to reach the nose of the animal. This latency was empirically estimated to be 70–100 ms using electro-olfactogram (EOG) as described in Uchida and Mainen (2003). Therefore, we corrected *odor sampling duration* by subtracting 100 ms to account for this delay. *Movement time* was defined as the time from withdrawal of the rat's snout out of the odor port to entry into one of the goal ports.

Neuronal Data Analysis

All data analysis was performed using MATLAB.

Epoch Definitions

After isolation of single cells, neuronal activity was analyzed in different task epochs. We divided the trial period into three epochs: stimulus, response, and outcome. The stimulus epoch was defined to begin with the odor valve opening (note that this definition does not take into account the odor latency to reach the epithelium; see Behavioral Analysis above) and end with response initiation (withdrawal from the odor port). The response epoch was defined to begin with response initiation and end with detection of entry into a goal port. The outcome epoch was defined as beginning with water valve onset for correct trials (or the maximum delay for error trials) and continuing for 500 ms. Firing rates were calculated during the entire duration of the stimulus, response, or outcome periods, except where noted.

Selectivity Analysis: Preference and Selectivity

To quantify selectivity for task variables (stimulus, response direction, outcome), we used an ideal observer decoding based on ROC analysis (Green and Swets, 1966). We defined relative *stimulus preference*: $\mathbf{p} = 2(ROC_{area} - 0.5)$, a measure with a range from −1 to 1, where −1 means "prefers B," 1 means "prefers A," and 0 represents no selectivity. This measure was also used to describe left versus right *direction preference* (right = −1, left = 1) and water delivery versus water omission *outcome preference* (no water = −1, water = 1). Absolute *selectivity* was defined as $\mathbf{s} = 2(|ROC_{area} - 0.5|)$, ranging from 0 to 1, where 0 means not selective, and 1 means selective for either condition (A or B, L or R, C or E). Note that this is just the absolute value of the preference defined above. Only cells with a minimum number of ten trials for each condition compared were included in this analysis. For stimulus selectivity within a response category in four-odor experiments, firing rates for trials of the two stimuli in each response category were compared using ROC analysis, as described above. In experiments with six odors, the firing rates of the three odors belonging to each response category were compared using a Kruskal-Wallis test (nonparametric ANOVA).

Choice Probability

Choice probability (Britten et al., 1996) is a metric based on ROC analysis that quantifies the ability to predict the rat's choice in a given trial by examining neuronal firing rates before the choice. It can be understood as the probability of, given the neuronal firing rate on a trial, correctly predicting the choice the rat makes. For each stimulus, we compared the firing rate at the end of the stimulus period (250 ms window preceding the movement out of the odor port) for trials in which the rat made a left or right choice (correct versus error). Cells were considered to show significant choice probability if left versus right trials could be distinguished for at least one of the stimulus conditions (cells that showed choice probability for both stimulus conditions were counted only once). To compute the mean choice probability, for each cell the highest choice probability (for A or B) was used.

Speed/Firing Rate and Speed/Temporal Width Correlations

Speed was calculated as: speed = distance/*movement time*, where distance was from the central port to the goal ports (57 mm). Firing was calculated using the end of the *response* period (a window of fixed length, 250 ms before entry into the goal port). For each direction-selective cell, firing rates in trials in the cell's preferred direction were correlated with the speed for the corresponding trials; the same was done for trials in the cell's nonpreferred direction. Thus, for each cell we obtained two correlation coefficients. Correlation coefficients were computed using the MATLAB routine *corrcoef*. This function tests the hypothesis of no correlation using t statistics. We report the p value resulting from that test.

Statistics

For all modulation, preference, and selectivity measurements (unless otherwise noted), significance was calculated using a permutation procedure. We used a criterion $p < 0.01$ to determine significance. At this level, five or six false positives are expected for an analysis of the entire population of 544 cells (and respectively fewer for analyses involving smaller populations).

All statistics reported are mean ± SEM, unless otherwise noted.

Supplemental Data

The Supplemental Data for this article can be found online at http://www.neuron.org/cgi/content/full/51/4/495/DC1/.

Acknowledgments

We would like to thank Drs. Christian Machens, Gidon Felsen, and Susana Lima Mainen for helpful comments on the manuscript. Support was provided by the National Institute on Deafness and Other Communication Disorders (5R01DC006104-02) as part of the NSF/NIH Collaborative Research in Computational Neuroscience Program (Z.F.M.), and fellowships from the Japan Society for the Promotion of Science (N.U.), and the Swartz foundation (N.U.). C.E.F. was the recipient of a George A. and Marjorie H. Anderson Fellowship at the Watson School of Biological Sciences.

Received: December 26, 2005
Revised: May 11, 2006
Accepted: June 30, 2006
Published: August 16, 2006

References

Arana, F.S., Parkinson, J.A., Hinton, E., Holland, A.J., Owen, A.M., and Roberts, A.C. (2003). Dissociable contributions of the human amygdala and orbitofrontal cortex to incentive motivation and goal selection. J. Neurosci. *23*, 9632–9638.

Britten, K.H., Newsome, W.t., Shadlen, M.N., Celebrini, S., and Movshon, J.A. (1996). A relationship between behavioral choice and the

visual responses of neurons in macaque MT. Vision Neuroscience *13*, 87–100.

Cacucci, F., Lever, C., Wills, T.J., Burgess, N., and O'Keefe, J. (2004). Theta-modulated place-by-direction cells in the hippocampal formation in the rat. J. Neurosci. *24*, 8265–8277.

Cardinal, R.N., Parkinson, J.A., Hall, J., and Everitt, B.J. (2002). Emotion and motivation: the role of amygdala, ventral striatum and prefrontal cortex. Neurosci. Biobehav. Rev. *26*, 321–352.

Carmichael, S.T., and Price, J.L. (1994). Architectonic subdivision of the orbital and medial prefrontal cortex in the macaque monkey. J. Comp. Neurol. *346*, 366–402.

Chen, L.L., Lin, L.H., Barnes, C.A., and McNaughton, B.L. (1994a). Head-direction cells in the trat posterior cortex. II. Contributions of visual and ideothetic information to the directional firing. Exp. Brain Res. *10*, 24–34.

Chen, L.L., Lin, L.H., Green, E.J., Barnes, C.A., and McNaughton, B.L. (1994b). Head-direction cells in the rat posterior cortex. I. Anatomical distribution and behavioral modulation. Exp. Brain Res. *101*, 8–23.

Cho, J., and Sharp, P.E. (2001). Head direction, place, and movement correlates for cells in the rat restrosplenial cortex. Behav. Neurosci. *115*, 3–25.

Corwin, J.V., Fussinger, M., Meyer, R.C., King, V.R., and Reep, R.L. (1994). Bilateral destruction of the ventrolateral orbital cortex produces allocentric but not egocentric spatial deficits in rats. Behav. Brain Res. *61*, 79–86.

Damasio, A.R. (1994). Descartes' error (New York: HarperCollins).

Dean, H.L., Crowley, J.C., and Platt, M.L. (2004). Visual and saccade-related activity in macaque posterior cingulate cortex. J. Neurophysiol. *92*, 3056–3068.

Dickinson, A., and Balleine, B.W. (1994). Motivational control of goal-directed behavior. Anim. Learn. Behav. *22*, 1–18.

Eichenbaum, H., Kuperstein, M., Fagan, A., and Nagode, J. (1987). Cue-sampling and goal-approach correlates of hippocampal unit activity in rats performing an odor-discrimination task. J. Neurosci. *7*, 716–732.

Ferino, F., Thierry, A.M., and Glowinski, J. (1987). Anatomical and electrophysiological evidence for a direct projection from Ammon's horn to the medial prefrontal cortex in the rat. Exp. Brain Res. *65*, 421–426.

Gallagher, M., McMahan, R.W., and Schoenbaum, G. (1999). Orbitofrontal cortex and representation of incentive value in associative learning. J. Neurosci. *19*, 6610–6614.

Gottlieb, J.P., Kusunoki, M., and Goldberg, M.E. (1998). The representation of visual salience in monkey parietal cortex. Nature *391*, 481–484.

Green, D.M., and Swets, J.A. (1966). Signal Detection Theory and Psycophysics (New York: Wiley).

Hafting, T., Fyhn, M., Molden, S., Moser, M.-B., and Moser, E.I. (2005). Microstructure of a spatial map in the entorhinal cortex. Nature *436*, 801–806.

Hasselmo, M.E. (2005). A model of prefrontal cortical mechanisms for goal-directed behavior. J. Cogn. Neurosci. *17*, 1115–1129.

Hok, V., Save, E., Lenck-Santini, P.P., and Poucet, B. (2005). Coding for spatial goals in the prelimbic/infralimbic area of the rat frontal cortex. Proc. Natl. Acad. Sci. USA *102*, 4602–4607.

Hyman, J.M., Zilli, E.A., Paley, A.M., and Hasselmo, M.E. (2005). Medial prefrontal cortex cells show dynamic modulation with the hippocampal theta rhythm dependent on behavior. Hippocampus *15*, 739–749.

Izquierdo, A., Suda, R.K., and Murray, E.A. (2004). Bilateral orbital prefrontal cortex lesions in rhesus monkeys disrupt choices guided by both reward value and reward contingency. J. Neurosci. *24*, 7540–7548.

King, V.R., Corwin, J.V., and Reep, R.L. (1989). Production and characterization of neglect in rats with unilateral lesions of ventrolateral orbital cortex. Experimental Neurology *105*, 287–299.

Kobayashi, S., Lauwereyns, J., Koizumi, M., Sakagami, M., and Hikosaka, O. (2002). Influence of reward expectation on visuospatial processing in macaque lateral prefrontal cortex. J. Neurophysiol. *87*, 1488–1498.

Koene, R.A., and Hasselmo, M.E. (2005). An integrate-and-fire model of prefrontal cortex neuronal activity during performance of goal-directed decision making. Cereb. Cortex *15*, 1964–1981.

Kolb, B., Sutherland, R.J., and Whishaw, I.Q. (1983). A comparison of the contributions of the frontal and parietal association cortex to spatial localization in rats. Behav. Neurosci. *97*, 13–27.

Leon, M.I., and Shadlen, M.N. (1999). Effect of expected reward magnitude on the response of neurons in the dorsolateral prefrontal cortex of the macaque. Neuron *24*, 415–425.

Lipton, P.A., Alvarez, P., and Eichenbaum, H. (1999). Crossmodal associative memory representations in rodent orbitofrontal cortex. Neuron *22*, 349–359.

Matsumoto, K., Suzuki, W., and Tanaka, K. (2003). Neuronal correlates of goal-based motor selection in the prefrontal cortex. Science *301*, 229–232.

McAlonan, K., and Brown, V.J. (2003). Orbital prefrontal cortex mediates reversal learning and not attentional set shifting in the rat. Behav. Brain Res. *146*, 97–103.

McCoy, A.N., Crowley, J.C., Haghighian, G., Dean, H.L., and Platt, M.L. (2003). Saccade reward signals in posterior cingulate cortex. Neuron *40*, 1031–1040.

McDannald, M.A., Saddoris, M.P., Gallagher, M., and Holland, P.C. (2005). Lesions of orbitofrontal cortex impair rats' differential outcome expectancy learning but not conditioned stimulus-potentiated feeding. J. Neurosci. *25*, 4626–4632.

McNaughton, B.L., Mizumori, S.J.Y., Barnes, C.A., Leonard, B.J., Marquis, M., and Green, E.J. (1994). Cortical representation of motion during unrestrained spatial navigation in rat. Cereb. Cortex *4*, 27–39.

Montague, P.R., and Berns, G.S. (2002). Neural economics and the biological substrates of valuation. Neuron *36*, 265–284.

Nitz, D.A. (2006). Tracking route progression in the posterior parietal cortex. Neuron *49*, 747–756.

O'Doherty, J., Kringelbach, M.L., Rolls, E.T., Hornak, J., and Andrews, C. (2001). Abstract reward and punishment representations in the human orbitofrontal cortex. Nat. Neurosci. *4*, 95–102.

O'Keefe, J., and Nadel, L. (1978). The Hippocampus as a Cognitive Map (Clarendon: Oxford, Oxford University Press).

Öngür, D., and Price, J.L. (2000). The organization of networks within the orbital and medial prefrontal cortex of rats, monkeys and humans. Cereb. Cortex *10*, 206–219.

Padoa-Schioppa, C., and Assad, J.A. (2006). Neurons in the orbitofrontal cortex encode economic value. Nature *441*, 223–226.

Pearce, J.M., and Hall, G. (1980). A model for Pavlovian learning: variations in the effectiveness of conditioned but not unconditioned stimuli. Psychol. Rev. *87*, 532–552.

Pickens, C.L., Saddoris, M.P., Setlow, B., Gallagher, M., Holland, P.C., and Schoenbaum, G. (2003). Different roles of orbitofrontal cortex and basolateral amygdala in a reinforcer devaluation task. J. Neurosci. *23*, 11078–11084.

Preuss, T.M. (1995). Do rats have prefrontal cortex? The Rose-Woolsey-Akert program reconsidered. J. Cogn. Neurosci. *7*, 1–24.

Reep, R.L., Corwin, J.V., and King, V.R. (1996). Neuronal connections of orbital cortex in rats: topography of cortical and thalamic afferents. Exp. Brain Res. *111*, 215–232.

Rescorla, R.A., and Wagner, A.R. (1972). A theory of Pavlovian conditioning: variations in the effectiveness of reinforcement and nonreinforcement. In Classical Conditioning II: Current Research and Theory, A.H. Black, ed. (New York: Appleton-Century-Crofts), pp. 64–99.

Roberts, A.C. (2006). Primate orbitofrontal cortex and adaptive behaviour. Trends Cogn. Sci. *10*, 83–90.

Roesch, M.R., and Olson, C.R. (2004). Neuronal activity related to reward value and motivation in primate frontal cortex. Science *304*, 307–310.

Roesch, M.R., and Olson, C.R. (2005). Neuronal activity in primate orbitofrontal cortex reflects the value of time. J. Neurophysiol. *94*, 1469–1497.

Rolls, E.T. (1996). The orbitofrontal cortex. Philos. Trans. R. Soc. Lond. B Biol. Sci. *351*, 1433–1443.

Rosenkilde, C.E., Bauer, R.H., and Fuster, J.M. (1981). Single cell activity in ventral prefrontal cortex of behaving monkeys. Brain Res. *209*, 375–394.

Samejima, K., Ueda, Y., Doya, K., and Kimura, M. (2005). Representation of action-specific reward values in the striatum. Science *310*, 1337–1340.

Schoenbaum, G., and Eichenbaum, H. (1995). Information coding in the rodent prefrontal cortex. I. Single-neuron activity in orbitofrontal cortex compared with that in pyriform cortex. J. Neurophysiol. *74*, 733–750.

Schoenbaum, G., and Setlow, B. (2001). Integrating orbitofrontal cortex into prefrontal theory: common processing themes across species and subdivisions. Learn. Mem. *8*, 134–147.

Schoenbaum, G., Chiba, A.A., and Gallagher, M. (1998). Orbitofrontal cortex and basolateral amygdala encode expected outcomes during learning. Nat. Neurosci. *1*, 155–159.

Schoenbaum, G., Chiba, A.A., and Gallagher, M. (1999). Neural encoding in orbitofrontal cortex and basolateral amygdala during olfactory discrimination. J. Neurosci. *19*, 1876–1884.

Schoenbaum, G., Nugent, S.L., Saddoris, M.P., and Setlow, B. (2002). Orbitofrontal lesions in rats impair reversal but not acquisition of go, no-go odor discriminations. Neuroreport *13*, 885–890.

Schoenbaum, G., Setlow, B., Nugent, S.L., Saddoris, M.P., and Gallagher, M. (2003a). Lesions of orbitofrontal cortex and basolateral amygdala complex disrupt acquisition of odor-guided discriminations and reversals. Learn. Mem. *10*, 129–140.

Schoenbaum, G., Setlow, B., Saddoris, M.P., and Gallagher, M. (2003b). Encoding predicted outcome and acquired value in orbitofrontal cortex during cue sampling depends upon input fromt basolateral amygdala. Neuron *39*, 855–867.

Schultz, W. (2002). Getting formal with dopamine and reward. Neuron *36*, 241–263.

Schultz, W., Tremblay, L., and Hollerman, J.R. (2000). Reward processing in primate orbitofrontal cortex and basal ganglia. Cereb. Cortex *10*, 272–283.

Sharp, P.E. (1999). Complimentary roles for hippocampal versus subicular/entorhinal place cells in coding place, context and events. Hippocampus *9*, 432–443.

Sutton, R.S., and Barto, A.G. (1998). Reinforcement Learning: An Introduction (Cambridge, MA: The MIT Press).

Swanson, L.W. (1998). Brain Maps: Structure of the Rat Brain, Second Edition (Amsterdam: Elsevier).

Taube, J.S. (1998). Head direction cells and the neurophysiological basis for a sense of direction. Prog. Neurobiol. *55*, 225–256.

Thorpe, S.J., Rolls, E.T., and Madison, S. (1983). The orbitofrontal cortex: neuronal activity in the behaving monkey. Exp. Brain Res. *49*, 93–115.

Tremblay, L., and Schultz, W. (1999). Relative reward preference in primate orbitofrontal cortex. Nature *398*, 704–708.

Tremblay, L., and Schultz, W. (2000a). Modifications of reward expectation-related neuronal activity during learning in primate orbitofrontal cortex. J. Neurophysiol. *83*, 1877–1885.

Tremblay, L., and Schultz, W. (2000b). Reward-related neuronal activity during go-nogo task performance in primate orbitofrontal cortex. J. Neurophysiol. *83*, 1864–1876.

Uchida, N., and Mainen, Z.F. (2003). Speed and accuracy of olfactory discrimination in the rat. Nat. Neurosci. *6*, 1224–1229.

Uylings, H.B.M., Groenewegen, H.J., and Kolb, B. (2003). Do rats have a prefrontal cortex? Behav. Brain Res. *146*, 3–17.

Vafaei, A.A., and Rashidy-Pour, A. (2004). Reversible lesion of the rat's orbitofrontal cortex interferes with hippocampus-dependent spatial memory. Behav. Brain Res. *149*, 61–68.

Wallis, J.D., and Miller, E.K. (2003). Neuronal activity in primate dorsolateral and orbital prefrontal cortex during performance of a reward preference task. Eur. J. Neurosci. *18*, 2069–2081.